Lithium-Fed Hollow Cathode Theory

Leonard D. Cassady* and Edgar Y. Choueiri†
Electric Propulsion and Plasma Dynamics Laboratory (EPPDyL)
Mechanical and Aerospace Engineering Department
Princeton University, Princeton, New Jersey 08544

AIAA-2004-3431‡
(Dated: July 11-14, 2004)

A theory for the single-channel hollow cathode (SCHC) that includes the relevant physical processes and predicts the operating parameters is presented. A SCHC consists of a cylindrical channel approximately ten diameters in length through which a working gas (taken as lithium vapor here) flows and exits as a plasma. A high current (1-100 A) is conducted into the channel by the plasma and to the cathode walls via field-enhanced thermionic emission and the plasma ions. The cathode voltage is determined from an energy balance that accounts for surface processes. An energy balance in the plasma volume determines the electron temperature. The SCHC theory includes, for the first time, a model of non-equilibrium excitation and ionization via thermionic and thermal electron collisions that utilizes a rate balance of the important excitation states of the lithium neutrals. The model predicts important operating parameters including the cathode voltage, temperature profile, and ionization fraction as a function of current, lithium flow rate, and channel diameter. The phenomenon of the minimum voltage as a function of current is captured by the model. The model gives insight into the primary loss mechanisms. It was found that thermal radiation dominates at low current, thermionic cooling dominates at moderate current, and convection of thermal electron energy dominates at high current.

I. INTRODUCTION

High-power electric propulsion systems have long been recognized as among the most promising options for heavy-payload orbit raising and piloted planetary missions [1–4], but research has been limited due to lack of in-space power. With NASA's renewed interest in the development of nuclear power systems for spacecraft, the steady-state power necessary for the practical application of these thrusters may soon be available. Among these high-power devices is the lithium Lorentz force accelerator (LiLFA), a type of magnetoplasmadynamic thruster (MPDT) that utilizes lithium propellant and a multichannel hollow cathode (MCHC). A MCHC is a single cathode that consists of several parallel SCHCs through which the propellant flows and current is conducted. Lithium is an ideal propellant for plasma thrusters where frozen flow losses are important, such as MPDTs, because of a low first ionization potential (5.4 eV), a high second ionization potential (75.6 eV), and a high first excitation level (61.95 eV) of Li II. The MCHC is critical to the LiLFA due to its dual purpose role of plasma source and arc cathode, yet there is no model that describes its operation.

A MCHC model requires the existence of a SCHC model and the inclusion of the thermal interaction of adjacent channels and the division of current and mass flow. In fact, there is no multichannel model that consistently includes ionization and current conduction. Ogarkov *et al.* [5, 6] studied MCHC design by focusing on plasma-surface interactions. The seminal work on MCHCs by Delcroix, Minoo, and Trindade [7] presented no detailed theory, instead their insightful analysis compares MCHC operation to that of a single-channel hollow cathode (SCHC).

Ferreira and Delcroix present the most detailed theory of the SCHC [9], however it required experimental data (the cathode temperature profile) as an input. Our goal is to develop a self-consistent SCHC model that will not require experimental data as an input, but rather that the predictions of the model can be compared to experimental data. To attain that goal, we are the first to include a model of non-equilibrium ionization and excitation via thermionic and thermal electron collisions that utilizes a rate balance of the important excitation states of the neutrals. We will extend our validated SCHC model to a MCHC model in the future.

In section II we present a self-consistent model that predicts the measurable properties of the cathode during operation as a function of the controllable parameters: the channel diameter, propellant mass flow rate, and current. The relevant measurable properties that

*Graduate Student, Former National Science and Engineering Graduate Fellow, Present Princeton Plasma Science and Technology Fellow; Electronic address: lcassady@princeton.edu
†Chief Scientist EPPDyL, Associate Professor, Applied Physics Group. Associate Fellow, AIAA.
‡Presented at the 40^{th} AIAA/ASME/SAE/ASEE Joint Propulsion Conference and Exhibit, Ft. Lauderdale, FL.

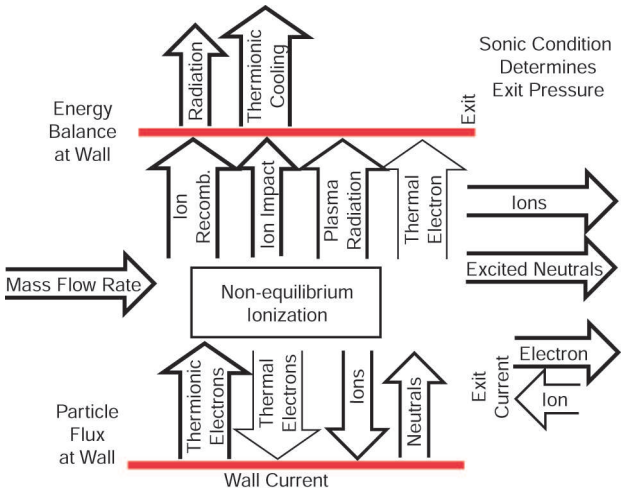

FIG. 1: Diagram of some of the processes in included in the SCHC model: the particle flux balance at the wall and through the channel, the energy balance at the wall, current conduction, and the ionization process.

our model will predict are the cathode voltage, electron temperature, and plasma ionization fraction. We present the results of the model and discuss the physical insights that our SCHC model provides in section III.

II. SCHC MODEL DESCRIPTION

A realistic physical model of the SCHC requires the inclusion of at least the following processes (shown in Fig. 1),

- Gas flow through the channel
- Non-equilibrium excitation/ionization
- Thermionic electron energy loss
- Work function reduction due to plasma sheath
- Current conduction at cathode
- Cathode heating
- Plasma electron heating

The channel of the hollow cathode is modelled as a cylinder of length l and radius r within which the plasma properties are assumed uniform, Fig. 2. The radius is an independent parameter that we choose according to experiments. The present model must use a plasma penetration depth l measured experimentally. We would rather determine l with the model, but we have not yet developed a theory for this process. We assume that the thermionic electrons are emitted from a uniform temperature tungsten wall that surrounds

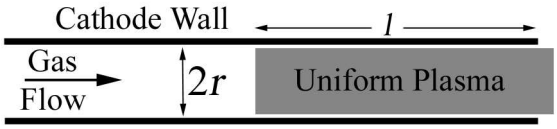

FIG. 2: Schematic of the cylindrical SCHC adopted for the model.

the channel. The number densities of the excited states of lithium and the thermionic electrons are determined by a rate balance of all of the collision and flow processes, assuming steady state.

A. Gas Flow

The plasma pressure within the channel is determined by the gas mass flow rate, the channel radius, cathode temperature, and velocity. The pressure outside of the channel is much less than that within and thus can be approximated as zero. The large pressure difference also implies a sonic condition at the cathode exit, which Ferreira and Delcroix [9] verified. The pressure at the exit of the channel is therefore determined by,

$$P_{ex} = \frac{\dot{m}}{\pi r^2}\sqrt{\frac{RT_c}{\gamma}} \tag{1}$$

where R is lithium's gas constant, T_c is the cathode temperature, and $\gamma = 5/3$ is the ratio of specific heats for a monatomic gas.

We will assume that the pressure along the channel is equal to P_{ex}. Using the theory of transitional channel flow presented by Dushman [10], the assumption is accurate to within a factor of three for the region within 10 channel diameters upstream of the exit.

Particle flux is conserved at the cathode wall and as the lithium vapor flows through the channel. The ions that impact the cathode wall are neutralized and return to the plasma volume as neutrals. The total flux of ions and neutrals leaving the cathode must match the flux of neutrals that enter the cathode.

B. Non-equilibrium Excitation/Ionization

The most important component of the SCHC model is non-equilibrium ionization. The lithium is ionized via multi-step inelastic collisions with beam electrons thermionically emitted from the cathode surface as well as thermal electrons in the plasma. Lithium excitation is accomplished primarily through collisions with the beam electrons. This forces a non-equilibrium model rather than Saha-type equilibrium model.

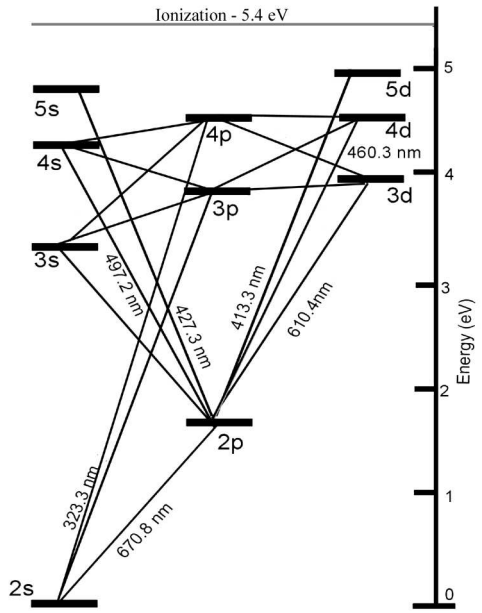

FIG. 3: Electronic levels of Li I adopted in the SCHC model, based on [11].

The collision frequencies are modelled utilizing experimental or theoretical cross-section data. The lowest eight states of neutral lithium and singly ionized lithium are included, as shown in Fig.3. The difference between the energies of the states above the 4d level is small compared to the energy associated with the electron temperature, therefore we can assume that the those states are easily ionized and do not require explicit modelling. A collision frequency is determined for each lithium state and beam electron energy.

1. Lithium Excitation Model

The state of the lithium neutral atom is modelled with electron-impact excitation transitions and spontaneous radiative emission of excited states of the atom. Published [12] values of the transition probability for spontaneous emission are used in the model. Since lithium has no metastable states, the forbidden transitions are not included in the excitation model. Also, no excited states of the lithium ion are considered since the first excited state is 61.95 eV.

The radiated power released by the spontaneous emission P_{sp} is partially trapped within the channel by the cathode walls. The radiated power that is not lost out of the end of channel heats the cathode surface. We will take the ratio of trapped to released radiation as the ratio of the sum of the channel exit and entrance areas to the total area surrounding the plasma volume,

$$R_{sp} = \frac{2\pi r^2}{2\pi r l + 2\pi r^2} = \frac{r}{l+r}. \tag{2}$$

The amount of power transferred to the cathode from the spontaneous emission process is $R_{sp}P_{sp}$, as required for the power balance in section II F.

2. Excitation and Ionization Via Thermionic Electrons

One of the two excitation and ionization processes is the inelastic collisions of mono-energetic electrons with the neutral lithium. Since we track the number density of beam electrons as a function of energy, we can calculate the collision frequency for the thermionic electrons as they decelerate. The frequency of a process p between the thermionic electrons (subscript th) and the state j of the lithium atom is

$$\nu^p_{th,j}(\epsilon) = n_j \sqrt{2\epsilon/m_e}\; Q^p_{th,j}(\epsilon), \tag{3}$$

where $Q^p_{th,j}(\epsilon)$ is the cross section of the process evaluated at the energy ϵ, n_j is the number density of the excited state j, and m_e is the electron mass. The processes are the various transitions between the states of lithium as well as ionizatoin. We have used the cross sections provided by the International Atomic Energy Agency [13] because they provide standardized formulae for electron impact cross sections as a function of energy.

3. Excitation and Ionization Via Thermal Electrons

The second excitation and ionization process is the collision of thermal electrons with the lithium atoms. Because of the relatively low excitation energies of lithium, even electrons with a low temperature can contribute significantly to ionization. The frequency of each transition is calculated from

$$\bar{\nu}^p_{p,j} = n_j \sqrt{\frac{2}{m_e}} \int_0^\infty \frac{2\epsilon\; Q^p_{th,j}(\epsilon)}{\sqrt{\pi}(kT_e)^{3/2}} \exp\left(-\frac{\epsilon}{kT_e}\right) d\epsilon, \tag{4}$$

where T_e is the electron temperature and k is the Boltzmann constant. These inelastic collisions drain power, P_{ex}, from the thermal electrons.

C. Thermionic Electron Energy Loss

We must account for the energy loss of the thermionic electrons as they collide with the electrons and neutrals in the plasma. The thermionic electrons enter the plasma with an energy equal to the sheath

voltage plus the initial thermal energy associated with the cathode temperature,

$$\epsilon_{th,i} = V_s + 3/2\ kT_c. \tag{5}$$

As discussed in Appendix A, the thermionic electrons have a Maxwellian energy distribution normal to the surface with an average equal to the cathode temperature [14–16] as they leave the surface. We can approximate the energy of the thermionic electrons as a mono-energetic beam because the energy gained by acceleration through the sheath is much greater than the energy associated with the surface temperature. Therefore, the energy differences due to the initial Maxwellian distribution are small compared to the energy gained by acceleration through the sheath and can be neglected.

Inelastic collisions with neutral lithium and elastic collisions with plasma electrons reduce the energy of the thermionic electrons until it is equal to the energy corresponding to the plasma temperature, at which point they are considered to be thermal plasma electrons. The energy lost in each inelastic collision is assumed to be equal to the energy of the excited state transition caused by the collision. The energy lost through collisions with plasma electrons is [17]

$$\Delta\epsilon_{th} = \frac{1}{2}\left(\epsilon_{th} - \frac{3}{2}kT_e\right). \tag{6}$$

We will call the total power lost P_h. This power heats the plasma electrons, as described in section II G.

D. Work Function Reduction Due to Plasma Sheath

The cathode wall and the internal plasma are separated by a sheath which accelerates the ions toward the wall and electrons into the plasma. The details of the sheath are not relevant with the exception of the electric field at the cathode surface because the field can reduce the effective work function. We use a version of the double sheath model developed by Prewett and Allen [18] modified to account for the finite energy of the thermionic electrons as they leave the cathode surface. Since our result is slightly different from previous researchers [16, 19] a derivation of the modified double sheath model is included in Appendix A. The electric field at the cathode surface, E_c, is determined by the relation

$$\begin{aligned}\frac{\epsilon_o}{2}E_c^2 &= -\frac{j_{th}m_e}{e}\left[\left(\frac{2e}{m_e}V_s + \frac{3kT_c}{m_e}\right)^{1/2} - \left(\frac{3kT_c}{m_e}\right)^{1/2}\right] \\ &+ 2n_{i,o}V_o e\left(\left(1+\frac{V_s}{V_o}\right)^{1/2} - 1\right) \\ &+ n_{e,o}kT_e\left(\exp\left(-\frac{eV_s}{kT_e}\right) - 1\right),\end{aligned} \tag{7}$$

where V_o represents the energy of the ions as they enter the sheath, $n_{i,o}$ and $n_{e,o}$ is the number density of the ions and electrons at the sheath/plasma boundary, ϵ_o is the permittivity of free space. The sheath voltage V_s is different from the cathode voltage due to the presheath potential required to accelerate the ions V_o,

$$V_s = V_c - V_o. \tag{8}$$

The reduction of the effective work function by the electric field (Schottky effect) is given by [20]

$$\phi_{eff} = \phi_o - \sqrt{\frac{eE_c}{4\pi\epsilon_o}}, \tag{9}$$

where ϕ_o is the work function of the cathode material.

E. Current Conduction at Cathode

Current is conducted from the plasma to the cathode via ions j_i, thermionic electrons j_{th}, and thermal electrons j_{pe} from the plasma,

$$\frac{J}{A_s} = j = j_{th} + j_i - j_{pe}, \tag{10}$$

where J is the total current and j is current density.

Thermal electron density follows a Boltzmann distribution determined by the potential in the sheath. The flux of electrons to the wall is then $\frac{1}{4}n_{pe,c}\bar{v}$ where $n_{pe,c}$ is the number density at the cathode and $\bar{v}$ is the average electron velocity as determined from the plasma electron temperature [21], therefore

$$j_{pe} = e\frac{1}{4}n_e\exp\left(-\frac{eV_s}{kT_e}\right)\left(\frac{8kT_e}{\pi m_e}\right)^{1/2}. \tag{11}$$

The thermionic current is described by the Richardson-Dushman equation [20],

$$j_{th} = AT_c^2\exp\left(-\frac{e\phi_{eff}}{kT_c}\right), \tag{12}$$

where A is an empirical constant for tungsten.

The ion current is determined from the ion flux as described in section II F,

$$j_i = en_i v_{B,m}. \tag{13}$$

We match the net current J to the desired current by adjusting the sheath voltage, which results in a change in cathode temperature and ionization fraction. Those changes are fed back iteratively into the thermionic and ion current allowing a solution to be found.

F. Cathode Heating

A power balance of the cathode is important because it determines the cathode temperature, which gives the thermionic current via the Richardson-Dushmann equation (12). The ions and electrons that bombard the surface and the spontaneous radiation supply energy while thermal radiation and thermionic cooling remove energy,

$$P_i + P_{pe} + P_{sp,c} = P_{rad} + P_{th}. \tag{14}$$

The power delivered by the ions has two components, the kinetic energy of impact and the energy released when the ion recombines with a surface electron to become a neutral,

$$P_i = n_i v_{B,m} \left(V_c - \phi_{eff} + \phi_i\right) A_s, \tag{15}$$

where $v_{B,m}$ is the modified Bohm velocity described in Appendix A and A_s area of the cathode wall.

If the plasma electron temperature is comparable to the cathode voltage then the electrons can reach the cathode and combine on the surface. The flux of electrons is given by equation (11) divided by e. If the voltage that corresponds to the electron temperature is less than sheath voltage, the average energy of each electron that reaches the cathode is

$$\bar{\epsilon}_{pe,c} = \frac{3}{2}\frac{kT_e}{e}. \tag{16}$$

Therefore, the power delivered by the thermal electrons is

$$P_{pe} = \frac{j_{pe}}{e}\left(\frac{3}{2}\frac{kT_e}{e} + \phi_{eff}\right) A_s, \tag{17}$$

where the energy released as the electrons recombine with the cathode material is included.

The spontaneous radiation emitted by the excited lithium atoms can be trapped within the channel, thus depositing power into the cathode wall. Using equation 2, we denote $P_{sp,c}$ as the spontaneous radiation power captured by the cathode as

$$P_{sp,c} = R_{sp} P_{sp}. \tag{18}$$

The thermal radiation is modelled using the Stefan-Boltzmann relation

$$P_{rad} = \epsilon_W \sigma T_c^4 A_s, \tag{19}$$

where ϵ_W is the emissivity of tungsten and σ is the Stefan-Boltzmann constant.

Finally, we include the power removed by thermionic cooling. As the electrons leave the cathode material they take energy that is equal to the sum of their initial temperature and the effective work function

$$P_{th} = j_{th} e \left(\phi_{eff} + 3/2\ kT_c\right) A_s. \tag{20}$$

G. Plasma Electron Heating

The temperature of the plasma electrons is determined by another power balance. The electron temperature is important because lithium excitation and ionization via thermal electrons depend strongly on that value. The plasma electrons gain energy through elastic collisions with the thermionic electrons. The energy is lost by transport out of the channel for current conduction, excitation and ionization of the lithium atoms, and conduction through to the cathode wall,

$$P_h = P_{ex}(T_e) + \frac{J_e}{e} kT_e + P_{pe}, \tag{21}$$

where we note that the power lost to excitation $P_{ex}(T_e)$ is a function of electron temperature and J_e is the total current conducted by the electrons out of the channel. We use this relation to self-consistently determine T_e.

III. RESULTS

A. Comparison with Experiment

We modelled a SCHC over a range of current at a fixed mass flow rate and channel diameter. Our goal was to demonstrate that the SCHC model can predict a minimum in the voltage, an increase in electron temperature, and an increase in ionization fraction as current is increased from 1 to 100 A, as observed experimentally by many researchers [5, 22–24]. (The following results were obtained from a simplified model that takes $P_{sp,c} = 0$ and $\phi_{eff} = \phi_o$. Those simplifications increase the predicted voltage 1-10% over the prediction of the complete SCHC model, but allow for results to be generated quickly. They have little effect on ionization fraction or electron temperature.)

We choose to compare our model to a single channel of a MCHC experiment conducted by Babkin *et al.* [25] because they measured voltage, ionization fraction, and electron temperature. Each channel diameter was 2 mm with an approximate mass flow rate of 0.1 mg/s, although the mass flow rate was probably lower due to the possibility of flow around the channels. It was noted that the plasma penetration depth was approximately one channel diameter, which we used as an input for the model.

The minimum cathode discharge voltage of 8 V occurred between 5-10 A per channel. The minimum predicted by the SCHC model was 6 V, a difference of only 2 V. The predicted voltage is within a factor of two of the experimental data across the entire range of measured current, shown in Fig. 4. The model predicted the minimum voltage at 30 A, which is off by a factor of three to six. This difference may be

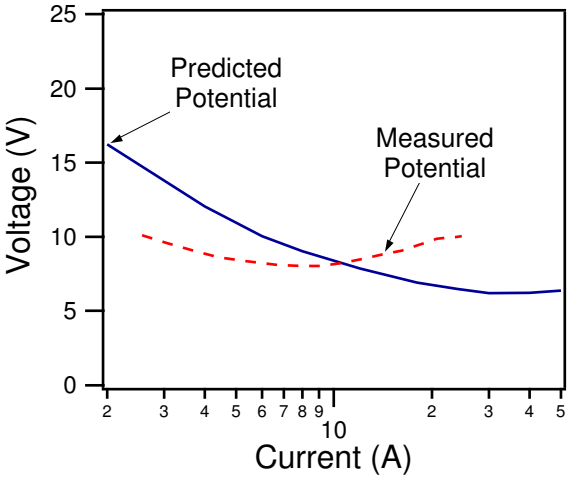

FIG. 4: A comparison of the predicted cathode voltage with experimental data. The measured potential represents 80% of the total discharge voltage as reported by Babkin *et al.* [25]

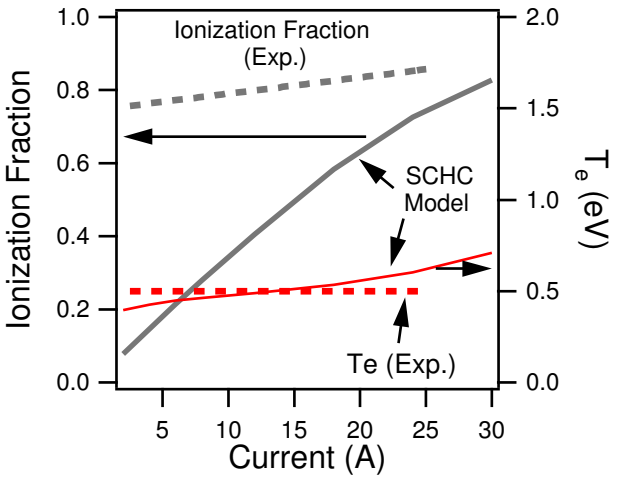

FIG. 5: A comparison of predicted electron temperature and ionization fraction with experimental data.

attributed to the reduced mass flow rate. Delcroix [8] demonstrated that a reduction in mass flow rate causes a reduction in the current at which the voltage is a minimum.

In Fig. 5 we show a comparison of electron temperature and ionization fraction. The measured temperature was approximately 0.5 eV while the model predicted an increase from 0.4 to 0.6 eV over the same range of current. Since no uncertainty was given for the measured electron temperature, we can not determine if the trend of increasing temperature predicted by the SCHC model is correct, although results from other experiments [22–24] show the trend predicted. The model predicts an ionization fraction that increases from 20% to 80% while it varied from 75% to 85% in the experiment. The trend of increasing ionization fraction with current is correct, but the prediction is off by a factor of four at low current. This difference may again be attributed to the reduced mass flow rate in each channel, which would increase the ionization fraction at a given current.

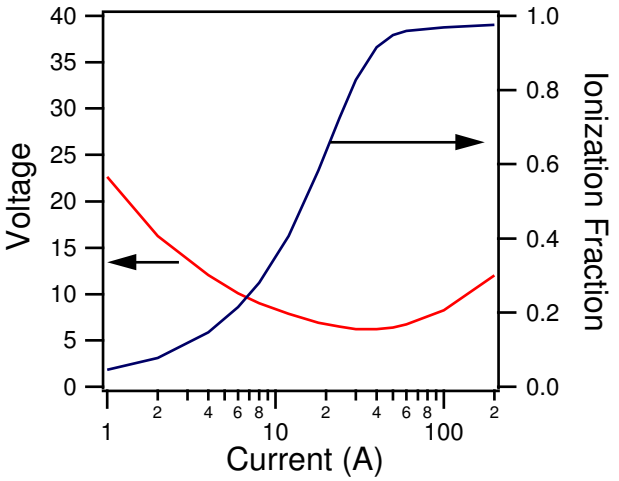

FIG. 6: SCHC model prediction of cathode voltage and ionization fraction.

B. Physical Insight

More importantly, the model also provides physical insight into the nature of the SCHC processes. As seen in Fig. 6, the minimum voltage occurs at a current that corresponds to an ionization fraction of 90%. An analysis of the primary power loss mechanisms provides further insight into SCHC operation as well as describing the minimum voltage phenomenon. It can be seen in Fig. 7 that at low current (<1 A) thermal radiation dominates the power loss mechanisms. As the current increases the power lost to thermionic cooling begins to dominate. This process dominates until the ionization fraction increases to approximately 90% (at 30 A), at which point the power lost to thermal electron convection begins to play a prominent role. The loss of power through convection is the factor that increases the voltage at high current. The electron temperature increases at a high ionization fraction because the thermal electrons have no neutral atoms to collide with inelastically to suppress their temperature. Also, at high current the flux of electrons is large and thus removes a large amount of power.

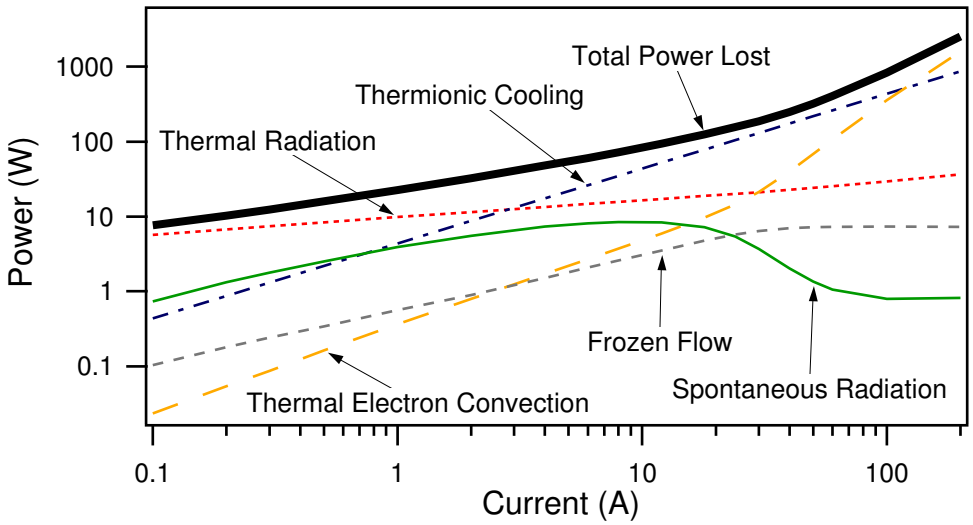

FIG. 7: SCHC model prediction of power loss mechanisms.

IV. CONCLUSION

We have presented a theory for the single-channel hollow cathode (SCHC) that includes the relevant physical processes and predicts the operating parameters of cathode voltage, temperature profile, and ionization fraction. The independent parameters of the model are current, lithium flow rate, and channel diameter. The SCHC theory includes, for the first time, a non-equilibrium excitation and ionization model of the working gas. As you have seen, the model:

- Captures the minimum voltage as a function of current that has been seen in experiments to within 2 V
- Predicts the trends of the voltage and electron temperature also seen in experiments
- Gives insight into the primary loss mechanisms. It was found that thermal radiation dominates at low current, thermionic cooling dominates at moderate current, and convection of thermal electron energy dominates at high current.

APPENDIX A: THE SHEATH MODEL

We begin by deriving a model of the double sheath, similar to that of Prewett and Allen [18]. We have included a finite thermal energy for the thermionic electrons, rather than the zero energy assumed by Prewett and Allen. At the high currents of a hollow cathode discharge the double sheath model of Prewett and Allen can predict a space charge limited current, which is not consistent with experimental results. Including a finite thermal energy gives a more accurate model of the sheath that results in larger values of the electric field at the cathode surface. In contrast to other researchers that included a finite thermal energy in their double sheath model [16, 19], we have set the average thermal energy to $\frac{3}{2}kT_c$.

A beam of electrons exit the cathode with a finite thermal energy and are accelerated through the sheath. Ions enter the sheath from the plasma and are accelerated until they reach the surface where they recombine to form neutrals. The contribution of the thermal electrons from the plasma is included as well. The cathode will be considered the origin of the problem and the plasma will be considered to have zero potential.

a. Thermionic Electrons

The thermionic electron flux is a fixed value determined by the temperature of the cathode. The electrons possess an initial thermal energy that is accurately described as a Maxwellian distribution [14, 15]. The average initial energy is thus directly related to the cathode temperature as $\frac{3}{2}kT_c$[17], where k is the Boltzmann constant. As stated in section II C, we can approximate the energy of the thermionic electrons as a mono-energetic beam because the energy gained by acceleration through the sheath is much greater than the energy associated with the surface temperature. Therefore, the energy differences due to the initial Maxwellian distribution are small compared to the energy gained by acceleration through the sheath and can be neglected. Energy conservation (assuming no collisions) gives the velocity of the thermionic electrons

as they pass through the sheath,

$$\frac{1}{2}m_e v_{th}^2 = e(V_s - V) + \frac{3}{2}kT_c, \tag{A1}$$

where $-V_s$ is the potential at the cathode, $-V$ is the potential through the sheath, e is the charge of an electron, m_e is the mass of an electron, and v_{th} is the velocity of the electron as it moves through the sheath.

The number density of the thermionic electrons can be found from continuity

$$n_{th} v_{th} = j_{th}/e, \tag{A2}$$

where n_{th} is the number density of thermionic electrons and j_{th} is the current density of the thermionic electrons. The number density is

$$n_{th} = \frac{j_{th}}{e} m_e^{1/2} \left[2e(V_s - V) + 3kT_c\right]^{-1/2}. \tag{A3}$$

b. Ions

The Bohm condition applies to the boundary between the sheath and the bulk plasma. The condition specifies that the ions enter the sheath with a velocity equal to the ion sound speed in the plasma. We will express the initial velocity, $v_{i,o}$, in terms of an equivalent potential, V_o,

$$\frac{1}{2}m_i v_{i,o}^2 = eV_o \tag{A4}$$

The energy of the ions can be expressed using the energy conservation equation

$$\frac{1}{2}m_i v_i^2 = \frac{1}{2}m_i v_{i,o}^2 + eV \tag{A5}$$

as they travel through the sheath without collisions. Combining equations A4 and A5 gives the ion velocity as a function of sheath potential

$$v_i = \left(\frac{2e}{m_i}\right)^{1/2} (V_o + V)^{1/2}. \tag{A6}$$

Again, the electrons must be conserved across the sheath

$$n_i v_i = n_{i,o} v_{i,o}, \tag{A7}$$

where $n_{i,o}$ is the number density of ions at the sheath edge. Combining equations A6 and A7 we get the relation for ion number density throughout the sheath

$$n_i = n_{i,o}(1 + V/V_o)^{-1/2}. \tag{A8}$$

c. Thermal Electrons

The thermal electrons within the plasma will penetrate the sheath by virtue of their high thermal energy. This is especially important for a lithium plasma sheath because the potential can be as little as 5 times the energy associated with the electron temperature. We will use a Boltzmann distribution to describe their energy distribution

$$n_e = n_{e,o}\ \exp\left(-eV/kT_e\right). \tag{A9}$$

d. Sheath Relations

Since we assumed that the sheath is not quasi-neutral we can use Poisson's equation to determine the potential within the sheath,

$$\epsilon_o \frac{d^2V}{dx^2} = \rho, \tag{A10}$$

where ϵ_o is the permittivity of free space and ρ is the space charge density. The space charge density in the sheath is determined by the sum of the relations we derived above for the thermionic electrons (A3), the ions (A8), and the thermal electrons (A9) multiplied by the electron charge,

$$\begin{aligned} \epsilon_o \frac{d^2V}{dx^2} &= -j_t m_e^{1/2} \left[2e(V_s - V) + 3kT_c\right]^{-1/2} \\ &+ n_{i,o} e (1 + V/V_o)^{-1/2} \\ &- n_{e,o} e\ \exp\left(-eV/kT_e\right). \end{aligned} \tag{A11}$$

We normalize the relation to clarify the fundamentals of the problem using the following normalized quantities:

$$\eta = \frac{eV}{kT_e} \tag{A12}$$

$$\tau = \frac{3T_c}{T_e} \tag{A13}$$

$$\nu_i = \frac{n_{i,o}}{n_{e,o}} \tag{A14}$$

$$J_{th} = \frac{j_{th}}{n_{e,o} e (kT_e/m_e)^{1/2}} \tag{A15}$$

$$\xi = x/\lambda_D \tag{A16}$$

$$\lambda_D = \left(\frac{\epsilon_o kT_e}{n_{e,o} e^2}\right)^{1/2}. \tag{A17}$$

The normalized equation is

$$\frac{d^2\eta}{d\xi^2} = \varrho = -J_{th}\left[2(\eta_c - \eta) + \tau\right]^{-1/2} + \nu_i(1 + \eta/\eta_o)^{-1/2} - \exp(-\eta). \quad \text{(A18)}$$

We can apply a boundary condition to the above equation to determine the value of one of the free parameters ν_i and η_o. Our first boundary condition is quasineutrality at the sheath-presheath boundary,

$$\varrho = 0 \text{ at } \eta = 0. \quad \text{(A19)}$$

This determines the value of the normalized ion density

$$\nu_i = 1 + J_{th}(2\eta_c + \tau)^{-1/2}. \quad \text{(A20)}$$

It can be seen that if there is no thermionic current the normalized ion density is unity, exactly the value predicted by Bohm for a space charge sheath.

The second boundary condition is derived by Andrews and Allen [18]

$$\frac{d\varrho}{d\eta} = 0 \text{ at } \eta = 0 \quad \text{(A21)}$$

and determines η_o

$$\eta_o = \frac{1}{2}\,\frac{1 + J_{th}(2\eta_c + \tau)^{-1/2}}{1 - J_{th}(2\eta_c + \tau)^{-3/2}}. \quad \text{(A22)}$$

Again, it can be seen that the Bohm condition is satisfied when the thermionic current is zero. These two boundary conditions can be thought of as modified Bohm conditions for an electron emitting cathode with a double sheath,

$$\frac{1}{2}m_i v_{B,m}^2 = \eta_o \frac{kT_e}{e}. \quad \text{(A23)}$$

The solution of the electric field is found by multiplying by dV/dx and integrating from x to the sheath edge. Setting $E = -dV/dx$, the result is

$$\epsilon_c^2 = -2J_{th}[(2\eta_c + \tau)^{1/2} - \tau^{1/2}] + 4\nu_i\eta_o[(1 + \eta_c/\eta_o)^{1/2} - 1] + 2\exp(-\eta_c) - 2 + \epsilon_e^2. \quad \text{(A24)}$$

An analysis of the normalized electric field will show that the ϵ_e term can be neglected. First, let's approximate the electric field E as $\Delta V/\Delta L$, where ΔL is the characteristic length of the presheath region

$$\epsilon_e = \frac{E\lambda_D}{kT_e/e} = \frac{\Delta V}{kT_e/e}\frac{\lambda_D}{\Delta L}. \quad \text{(A25)}$$

The characteristic length is defined by the mean free path of the ions, which is normally 10^2 to 10^3 times greater than the Debye length. If we consider that the field in the presheath is the largest near the sheath, conservatively an order of magnitude larger, we can approximate $\Delta L \approx 10\lambda_D$. The voltage fall in the presheath is approximately half of the electron temperature

$$\frac{\Delta V}{kT_e/e} \approx \frac{1}{2}, \quad \text{(A26)}$$

which gives

$$\epsilon_e = \frac{\lambda_D}{2\ \Delta L} \approx \frac{1}{20}. \quad \text{(A27)}$$

In equation A24 the electric field at the presheath boundary is squared. The square of our approximation of $\epsilon_e^2 = 1/400$ is much smaller than 2, thus it will be neglected.

The electric field at the cathode surface will be determined from

$$\epsilon_c^2 = -2J_{th}[(2\eta_c + \tau)^{1/2} - \tau^{1/2}] + 4\nu_i\eta_o[(1 + \eta_c/\eta_o)^{1/2} - 1] + 2\exp(-\eta_c) - 2. \quad \text{(A28)}$$

e. Presheath effects

We use a simple approximation for the voltage drop across the presheath that is based solely on the Bohm velocity. There are two reasons for using a simple approximation: 1) no analytical solution is possible for the case of thermionically emitting cathode and 2) the presheath has little bearing on the hollow cathode physics. The presheath voltage will be taken as η_o from equation A22.

It is difficult to develop an accurate theory to describe the acceleration of the ions to the Bohm velocity because only a few simple cases are solvable analytically [26]. Presheaths that are dominated by collisions or ionization have voltages of 0.6 kT_e/e [27] or 0.69 kT_e/e [26, 28], respectively. Neither case is appropriate, but they demonstrate the small range of presheath potentials.

[1] R. Frisbee. SP-100 nuclear electric propulsion for mars cargo missions. In *29th AIAA/SAE/ASME/ASEE Joint Propulsion Conference*, Monterey, CA, USA, June 1993. AIAA-93-2092.

[2] R. Frisbee. Electric propulsion options for mars cargo missions. In *32nd AIAA/ASME/SAE/ASEE Joint Propulsion Conference and Exhibit*, Lake Buena Vista, FL, USA, July 1996. AIAA-96-3173.

[3] J. Polk. Alkali metal propellants for MPD thrusters. In *AIAA/NASA/OAI Conference on Advanced SEI Technologies*, Cleveland, OH, USA, September 1991. AIAA-91-3572.

[4] K. Sankaran, L.D. Cassady, A.D. Kodys, and E.Y. Choueiri. A survey of propulsion options for cargo and piloted missions to mars. In E. Belbruno, D. Folta, and P Gurfil, editors, *Astrodynamics Space Missions and Chaos*, volume 1017, pages 450–567, New York, NY, USA, 2004. Annals of the New York Academy of Sciences.

[5] V.M. Ogarkov, S.N. Ogorodnikov, and V.N. Stepanov. The design of the multirod cathode of a high-current plasma source. *Radio Engineering and Electronic Physics-USSR*, 21(12):98–103, 1976.

[6] V.M. Ogarkov, S.N. Ogorodnikov, and V.N. Stepanov. The influence adsorption effects on the characteristics of a high-current multirod cathode. *Radio Engineering and Electronic Physics-USSR*, 23(8):123–127, 1979.

[7] J.L. Delcroix, H. Minoo, and A.R. Trindade. Gas fed multichannel hollow cathode arcs. *Review of Scientific Instruments*, 40(12):1555–1562, December 1969.

[8] J.L. Delcroix and A.R. Trindade. *Advances in Electronics and Electron Physics*, volume 35, chapter Hollow Cathode Arcs, pages 87–190. Acedemia Press, New York, NY, USA, 1974.

[9] C.M. Ferreira and J.L. Delcroix. Theory of the hollow cathode arc. *Journal of Applied Physics*, 49(4):2380–2395, April 1978.

[10] S. Dushman. *Scientific foundations of vacuum technique*. John Wiley, New York, NY, USA, 1949.

[11] J.W. Turkstra. *Hot recoils from cold atoms*. Ph.d. thesis, RIJKSUNIVERSITEIT GRONINGEN, October 2001.

[12] W.L. Wiese, M.W. Smith, and B.M. Glennon. *Atomic Transition Probabilities*. Number 4 in National Standard Reference Data Series. National Bureau of Standards, Washington, DC, May 1966.

[13] Nuclear Data Section/Atomic International Atomic Energy Agency and Molecular Data Unit. ALLADIN database. Web Site: http://gap3.lpgp.u-psud.fr/GENIE/, 2004.

[14] T.J. Jones. *Thermionic Emission*. Methuen & Co, Ltd., London, England, 1936.

[15] A.L. Reimann. *Thermionic Emission*. John Wiley & Sons, Inc., New York, NY, USA, 1934.

[16] X. Zhou and J. Heberlein. Analysis of the arc-cathode interaction of free-burning arcs. *Plasma Sources Science and Technology*, 3(4):564– 574, November 1994.

[17] M. Mitchner and C.H Kruger. *Partially Ionized Gases*. John Wiley & Sons, Inc., New York, NY, USA, 1973.

[18] P.D. Prewett and J.E. Allen. The double sheath associated with a hot cathode. *Proceedings of the Royal Society of London Series A, Mathematical and Physical Sciences*, 348(1655):435–446, 1976.

[19] K.D. Goodfellow and J.E. Polk. High current cathode thermal behavior, part 1: Theory. In *23rd International Electric Propulsion Conference*, Seattle, WA, USA, September 1993. AIAA/AIDAA/DGLR/JSASS. IEPC-93-030.

[20] J.D. Cobine. *Gaseous Conductors*. Dover, New York, 1958.

[21] B. Rethfeld, J. Wendelstorf, T. Klein, and G. Simon. A self-consistent model for the cathode fall region of an electric arc. *Journal of Physics D: Applied Physics*, 29(1):121–128, January 1996.

[22] G.V. Babkin, V.G. Mikhalev, S.N. Ogorodnikov, R.V. Orlov, and A.V. Potapov. High-current coaxial plasma source. *Soviet Physics - Technical Physics*, 20(9):1175–1178, 1976.

[23] G.A. Dyuzhev, E.A. Startsev, and V.G. Yur'ev. Physics of a hollow arc cathode with a highly ionized dense plasma. *Soviet Physics - Technical Physics*, 23(10):1157–1163, October 1978.

[24] F.G. Baksht and A.B. Rybakov. Arc mode in a flow-through hollow cathode. *Soviet Physics - Technical Physics*, 23(4):412–415, April 1978.

[25] G.V. Babkin, V.G. Mikhalev, E.P. Morozov, and A.V. Potapov. An experimental investigation of a plasma in a multichannel cathode. *Journal of Applied Mechanics and Technical Physics*, 17(6):767–770, 1976.

[26] K.U. Riemann. The Bohm criterion and sheath formation. *Journal of Physics D: Applied Physics*, 24(4):493–517, April 1991.

[27] K.U. Riemann. Kinetic theory of the plasma sheath transition in a weakly ionized plasma. *Physics of Fluids*, 24(12):2163–2172, December 1981.

[28] G.S. Kino and E.K. Shaw. Two-dimensional low-pressure discharge theory. *The Physics of Fluids*, 9(3):587–593, March 1966.